

This is a repository copy of Itaconate utilisation by the human pathogen Pseudomonas aeruginosa requires uptake via the IctPQM TRAP transporter.

White Rose Research Online URL for this paper: https://eprints.whiterose.ac.uk/id/eprint/233260/

Version: Published Version

Article:

Mehboob, Javeria, Herman, Reyme, Elston, Rory C et al. (5 more authors) (2025) Itaconate utilisation by the human pathogen Pseudomonas aeruginosa requires uptake via the IctPQM TRAP transporter. The Biochemical journal. ISSN: 1470-8728

https://doi.org/10.1042/BCJ20253132

Reuse

This article is distributed under the terms of the Creative Commons Attribution (CC BY) licence. This licence allows you to distribute, remix, tweak, and build upon the work, even commercially, as long as you credit the authors for the original work. More information and the full terms of the licence here: https://creativecommons.org/licenses/

Takedown

If you consider content in White Rose Research Online to be in breach of UK law, please notify us by emailing eprints@whiterose.ac.uk including the URL of the record and the reason for the withdrawal request.







Research

Itaconate utilisation by the human pathogen Pseudomonas aeruginosa requires uptake via the IctPQM TRAP transporter

Javeria Mehboob^{1,2*}, Reyme Herman^{1,2*}, Rory C. Elston^{1,2}, Heritage Afolabi¹, Bethan E. Kinniment-Williams^{2,3}, Marjan W. van der Woude^{2,3}, Anthony J. Wilkinson⁴ and Gavin H. Thomas^{1,2}

Department of Biology, University of York, Wentworth Way, York, Y010 5DD, U.K; York Biomedical Research Institute, University of York, Y010 5DD, U.K; Hull York Medical School, University of Hull, Hull, Hu6 7RX, U.K; York Structural Biology Laboratory, Department of Chemistry, University of York, York, Y010 5DD, U.K

Correspondence: Gavin H. Thomas (gavin.thomas@york.ac.uk)



Pseudomonas aeruginosa PA01 is one of the major causes of disease persistence and mortality in patients with lung pathologies, relying on various host metabolites as carbon and energy sources for growth. The ict-ich-ccl operon (pa0878, pa0882 and pa0883) in PAO1 is required for growth on the host molecule itaconate, a C5-dicarboxylate. However, it is not known how itaconate is taken up into P. aeruginosa. Here, we demonstrate that a genetically linked tripartite ATP-independent periplasmic (TRAP) transporter (pa0884pa0886), which is homologous to the known C4-dicarboxylate-binding TRAP system, is essential for growth on itaconate, but not for the closely related C₄-dicarboxylate succinate. Using tryptophan fluorescence spectroscopy, we demonstrate that the substrate-binding protein (SBP), IctP (PA0884), binds itaconate but still retains higher affinity for the related C₄-dicarboxylates. The structures of IctP bound to itaconate (1.80 Å) and succinate (1.75 Å) revealed an enclosed ligand-binding pocket with ion pairing interactions with the ligand carboxylates. The C2 methylene group that is the distinguishing feature of itaconate compared with succinate is accommodated by a unique change in the IctP-binding site from a Leu to Val, which distinguishes it from closely related C₄-dicarboxylate-binding SBPs. Together, these data suggest that this transporter, which we name lctPQM, has duplicated from a canonical C₄-dicarboxylate transporter, and its evolution towards itaconate specificity enables this pathogen to now access a key metabolite for persistence in the host.

Introduction

Pseudomonas aeruginosa (P. aeruginosa) is a Gram-negative biofilm-forming opportunistic pathogen, which is one of the major causes of pulmonary pathologies, pneumonia, bacteraemia and other nosocomial infections [1]. This species accounts for around 7% of nosocomial infections [2,3] and, due to increasing antimicrobial resistance, is classified among the WHO priority pathogens [4]. P. aeruginosa has been linked with high morbidity and mortality in patients suffering from chronic infections that exhibit bacterial persistence, such as idiopathic pulmonary fibrosis [5], cystic fibrosis (CF) [6], asthma [7] and chronic obstructive pulmonary disease (COPD) [8]. During infection, P. aeruginosa adapts to the environment of the host by regulating the expression of virulence factors such as the polysaccharide alginate, outer-membrane proteins and its secretion system for flagella and pili. These factors allow the bacterial cell to survive by adhesion and colonisation of host cells and contribute to chronic infection [9,10].

In addition to cell surface factors, bacteria able to compete and colonise niches like the CF lung need to access carbon and energy sources to facilitate growth. *P. aeruginosa* has been known for a long time to prefer short-chain dicarboxylates over other more commonly favoured carbon and energy sources like glucose, and possesses a regulatory cascade that reflects this [11]. Colonisation by pathogens of other human niches like the gut relies on efficient use of host and dietary carbohydrates such as glucose [12], fucose [13,14] and sialic acid [15], while the regulatory hierarchy of *P. aeruginosa* suggests that this is not a niche in which it would be competitive. The particular ability of *P. aeruginosa* to be a regular extracellular coloniser of the CF lung is not totally understood. Emerging evidence suggests that the loss of the CF transmembrane conductance regulator results in wider metabolic dysregulation and secretion of the C₄-dicarboxylate succinate leading to longer-term infections [16]. Interestingly, when *P. aeruginosa* consumes succinate, this then triggers the host to release the related compound itaconate,

*These authors contributed equally to this work.

Received: 1 April 2025 Revised: 1 August 2025 Accepted: 7 August 2025

Version of Record Published: 2 September 2025



2-methylenesuccinate [16], which facilitates the characteristic chronic infection [17]. While succinate can be directly incorporated into central metabolism, the more unusual C_5 -dicarboxylate itaconate requires the products of the *ict-ich-ccl* genes (PA0878, PA0882 and PA0883) to catabolise it to pyruvate and acetyl-CoA [18,19].

Bringing these negatively charged metabolites into PA01 requires active transport by two transporters, DctA and DctPQM, which are involved in the uptake of C₄-dicarboxylates [20]. They appear to provide the only route for uptake of malate and fumarate, while residual uptake of succinate suggests that an additional system(s) is present [20]. In addition to DctPQM, P. aeruginosa PAO1 contains three other DctP-family tripartite ATP-independent periplasmic transporters (TRAP) [21], two of which are phylogenetically closely related to DctPQM (PA5167-9), the closest being that encoded by the pa0884-6 genes [21]. This system is the uncharacterised TRAP transporter that is encoded immediately downstream of the itaconate catabolic genes with PA0884 being the substrate-binding protein (SBP) and PA0885-6 being the small and large membrane subunits, respectively [21]. As part of work on the catabolic enzymes in P. aeruginosa strain PA14, the pa0886 gene was disrupted, and growth on itaconate was reduced compared with the wildtype (WT) [19], which combined with its location within the itaconate utilisation operon in PAO1 strongly suggests a function in itaconate transport [19,20,22]. Furthermore, the introduction of the whole region, including the transporter and the associated itaconate catabolic genes into the related bacterium P. putida allowed the latter to grow on itaconate, supporting the idea that PA0884-6 is an itaconate-specific TRAP transporter [23]. In this study, we combine genetic, biochemical and structural approaches to characterise this transporter, which we call IctPQM following the regular naming pattern for TRAP transporters and discover how P. aeruginosa has evolved a new transporter through duplication and specialisation towards itaconate over other C4-dicarboxylates, which enable it to utilise a key host molecule.

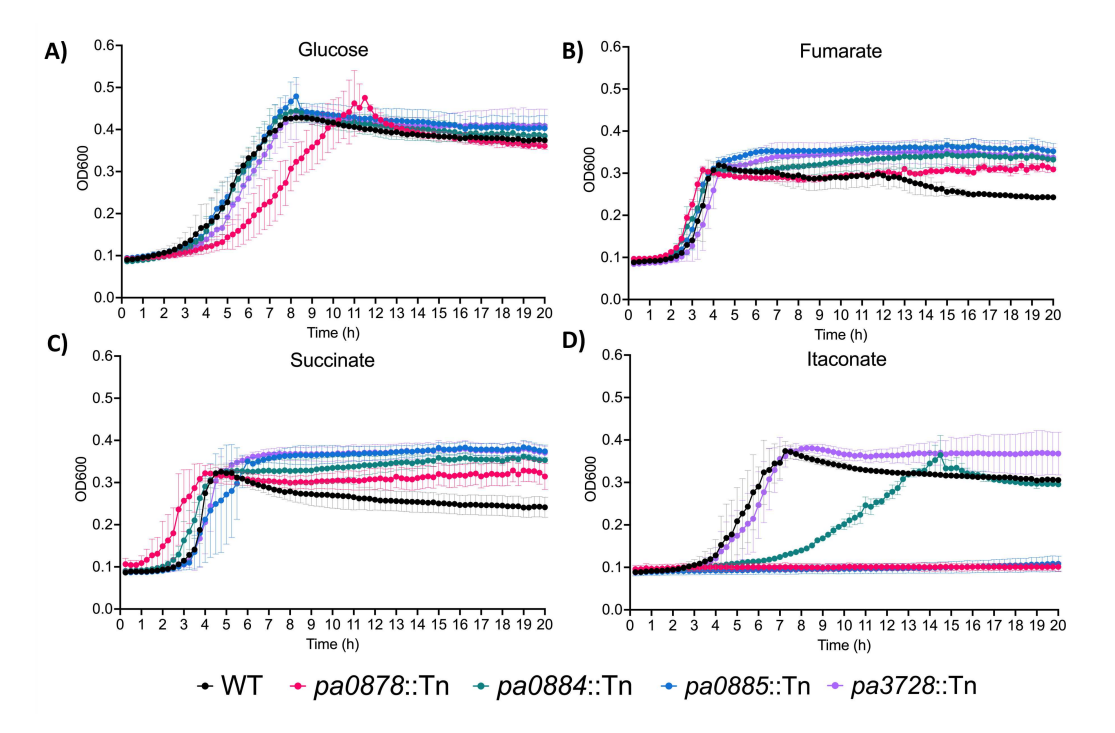


Figure 1: Growth curves of wild type and mutant *P. aeruginosa* strains in minimal media containing 5 mM of the indicated carbon sources.

(A) D-glucose, (B) fumarate, (C) succinate, (D) itaconate. Data were collected for three biological replicates. WT, wildtype.



Results

The PA0884-6 TRAP transporter is essential for growth on itaconate

To investigate whether the PA0884-6 TRAP transporter has a role in the physiological uptake of itaconate, we measured growth of the WT strain and isogenic mutants disrupted in *pa0884* (SBP) and *pa0885* (small membrane subunit) in minimal media supplemented with 5 mM of different carbon and energy sources (Figure 1). As controls, we also included a strain from the same mutant library with a disruption in an unrelated gene (*pa3728*) and a strain with a disruption in a gene encoding an essential component of the itaconate catabolic cluster (*pa0878*) [22]. All strains grow well with glucose, although the *pa0878* mutant appears to have a small growth reduction, which is similar to the phenotype observed in a previous study [19]. All strains grow well on succinate and fumarate, with more rapid initial growth than with glucose, reflecting the known preference for C₄-dicarboxylates as carbon sources [20,24,25]. Importantly, with itaconate as the carbon source, the pattern is different with no growth for the *pa0878* catabolic mutant as expected, but also no growth for the *pa0885* mutant in the TRAP transporter membrane domain. This is consistent with a previous disruption in *pa0886*, the large membrane subunit of the transporter [19]. However, somewhat surprisingly, the *pa0884* mutant gives an intermediate phenotype with an increased lag and reduced growth rate (Figure 1D) suggesting that there may be another closely related SBP that binds

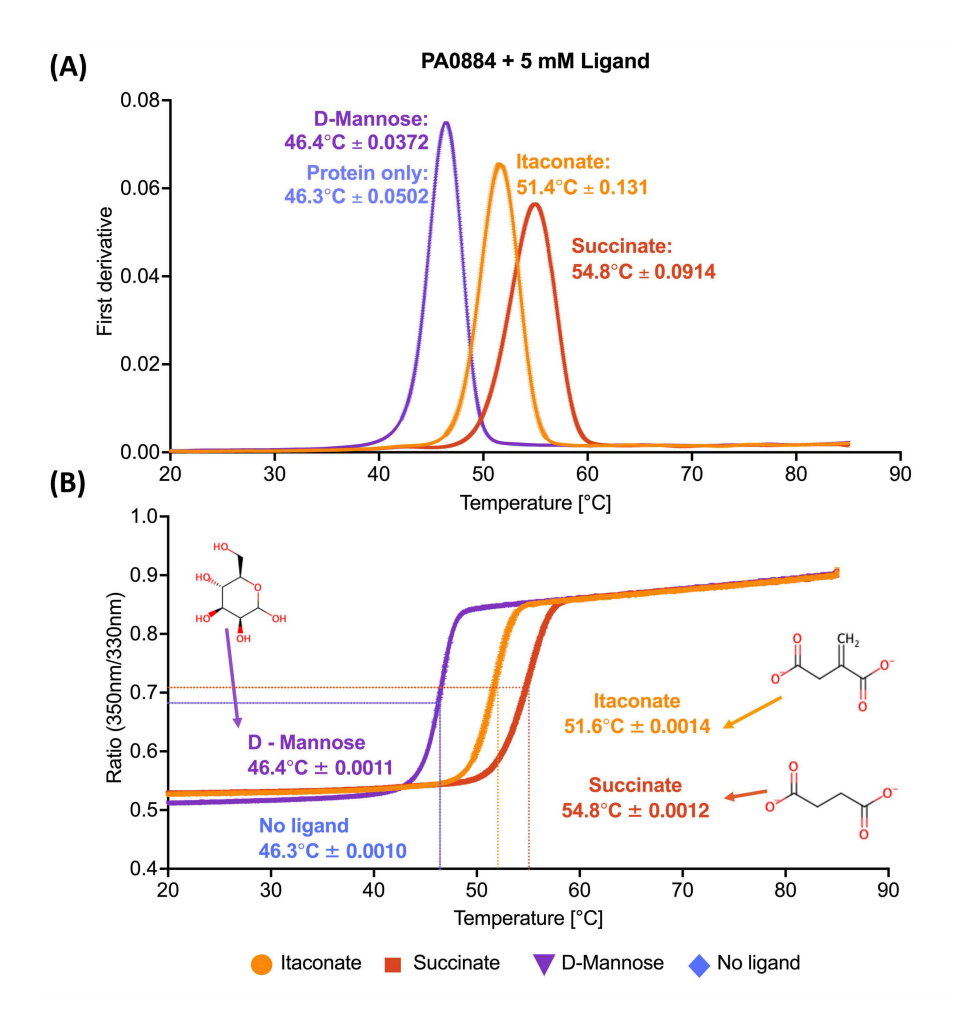


Figure 2: NanoDSF analysis of ligand binding to IctP (PA0884).

The plots show in (**A**) the first derivative and (**B**) the corresponding ratio of 350/330 nm traces in the presence of 5 mM itaconate, succinate and σ -mannose. The negative control contained protein in the absence of any ligand. Structures of each ligand are included in both figures along with the Tm + / - standard deviation (SD) for the three technical repeats.



to itaconate. On the basis of this *in vivo* phenotype, we suggest, following the standard naming conventions for TRAP transporters, that this system is called the IctPQM TRAP transporter.

IctP (PA0884) can interact with C₄-dicarboxylates similar in structure to succinate, including the airway metabolite itaconate

To biochemically assess the ability of the PA0884-PA0886 TRAP system in PAO1 to recognise dicarboxylates relevant to colonisation of the CF lung, we assessed their binding to recombinantly expressed IctP (PA0884) (Supplementary Figure S1), the SBP of the transport system, using nano differential scanning fluorimetry (nanoDSF) (Figure 2A). During purification, recombinantly expressed PA0884 was first partially unfolded with guanidine hydrochloride to remove any endogenous ligand likely to be present before being refolded. Upon addition of the airway metabolites succinate and itaconate to IctP, we observed an increase in thermal stability of the protein by ~8.5°C and ~5°C, respectively (Figure 2B), whereas the sugar D-mannose gave no or very small shifts similar to no ligand control. These data provide the first biochemical suggestions that succinate and itaconate bind directly to IctP.

IctP can bind to itaconate but is not its preferred ligand

We next determined the binding affinities of the SBP and various ligand interactions using intrinsic fluorescence spectroscopy (Figure 3). Following a similar pattern to the nanoDSF, both itaconate and succinate were bound by IctP, with respective binding affinities of 179.6 μ M±17.1 μ M and 32.6 μ M±1.5 μ M, supporting the finding that succinate exhibits tighter binding to the protein. In fact, when examining the binding of two other C₄-dicarboxylates that are recognised by DctP-like SBPs, namely L-fumarate and L-malate, we found that L-malate exhibited tightest binding with a K_D of 16.2 μ M±1.5 μ M. Our biochemical analysis suggests that while PA0884 can bind itaconate, it still has retained strong binding for the regular C₄-dicarboxylates.

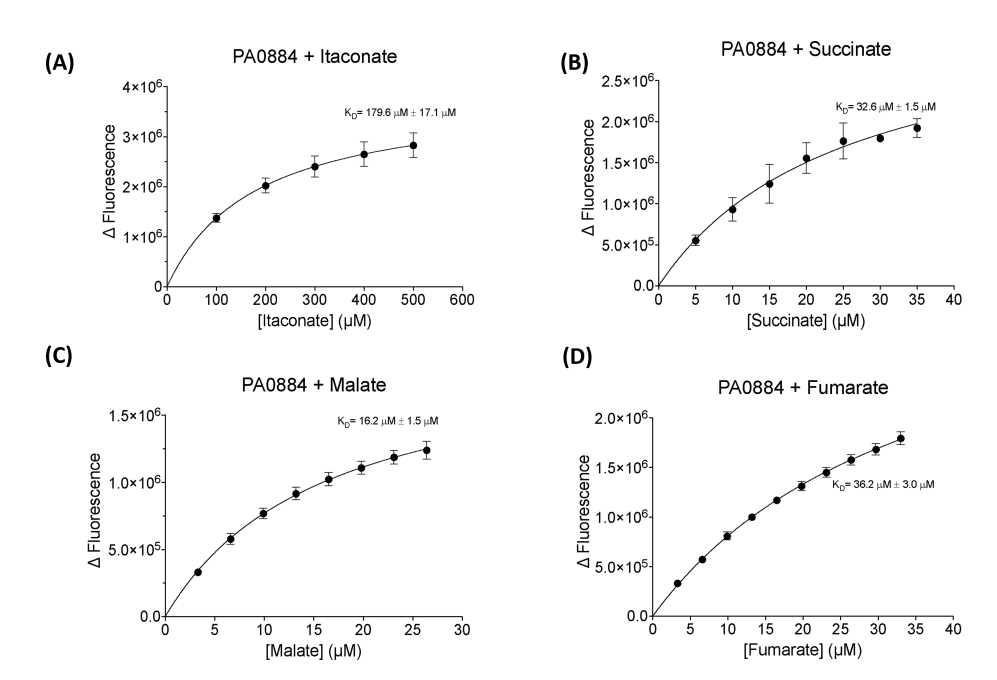


Figure 3: Investigation of ligand-binding affinities of IctP (PA0884) to dicarboxylate ligands through measuring changes in intrinsic protein fluorescence.

Intrinsic fluorescence was measured at 295/330 nm with ligand titrations (A) itaconate, (B) succinate, (C) malate and (D) fumarate. Standard deviations are shown for the KD values.



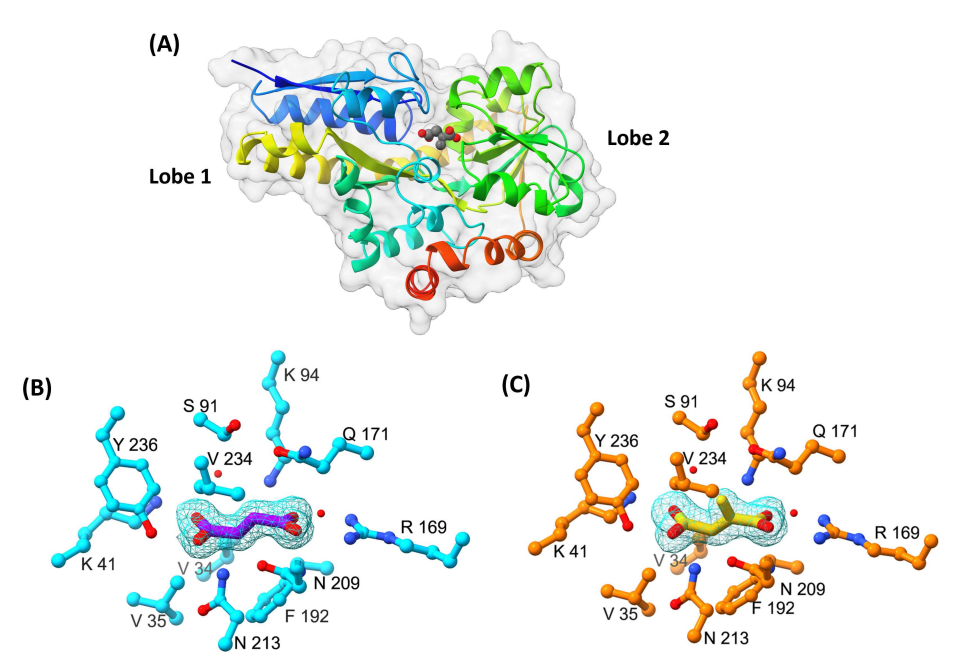


Figure 4: Structural characterisation of IctP with bound ligands.

(A) Ribbon tracing of the backbone of PA0884 colour ramped from the amino terminus (blue) to the C-terminus (red). The enclosed itaconate ligand is shown in sphere format coloured by atoms with carbons in grey and oxygens in red. A transparent protein surface emphasises the burial of the ligand. (B) Electron density map (2Fo—Fc) of the itaconate ligand (yellow) in PA0884 (orange) (contour level=0.3).

Itaconate is accommodated within an expanded hydrophobic pocket in the binding site of IctP

To reveal the molecular basis of binding for the dicarboxylates tested, we determined crystal structures of IctP in complexes with itaconate (PDB: 9HT3) and succinate (PDB: 9HT4) [26]. Both structures reveal the protein to be in a closed ligand-bound form similar to that seen for other TRAP SBPs [27–31] comprising two lobes (Figure 4A) with the ligands buried in an enclosed binding site. The itaconate ligand fulfils its hydrogen bonding and electrostatic potential through extensive interactions of its carboxylate groups (Supplementary Figure S2A,B), both of which are expected to be ionised (pKa values of 3.8 and 5.5) at the pH of crystallisation. The proximal (C1) carboxylate group forms a two-pronged ion-pair with the guanidino moiety of R169, a key characteristic of a DctP family SBP ligand interaction [32,33], further interacting with the ε-amino group of K94, the amide –NH₂ of N209 and an ordered water molecule (Figure 4B). Meanwhile, the distal (C4) carboxylate forms polar interactions with the charged amino group

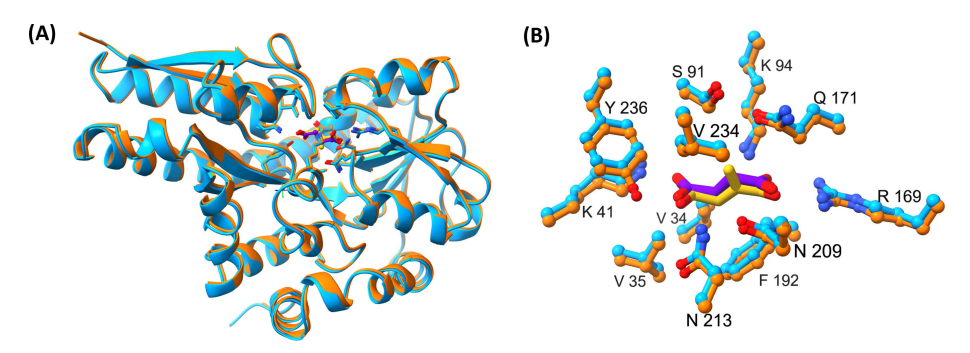


Figure 5: Structural alignments of PA0884 in complex with itaconate and succinate.

(A) Overlay of PA0884 bound to succinate (cyan) and PA0884 bound to itaconate (orange). (B) A close-up view of the ligand-binding site of PA0884 (cyan) bound to succinate (purple) and PA0884 (orange) bound to itaconate (yellow). Alignment algorithm used is Needleman—Wunsch and the similarity matrix is BLOSUM-62.



of the K41 side chain, the amide $-NH_2$ moiety of the side chain of N213, the phenolic hydroxyl of Y236 and a further ordered water molecule. These polar interactions are supplemented by apolar interactions involving the side chains of V34, V35, S91, F192 and V234. The nearest neighbours of the methylene substituent are provided by the side chains of Q171, V234 and S91. This group is otherwise enclosed by the K94 side chain and a water molecule.

For the succinate complex, the ligand occupies a similar volume to the itaconate, and the structure of the surrounding residues is essentially unchanged (Figure 4C). As a result, the carboxylate groups form the same set of strong polar interactions with protein side chains as described for itaconate (Figure 5AB). For both ligands, the C4 carboxylates are directed into lobe 1, while the C1 carboxylates project towards lobe 2. The formation of these interactions would therefore be accompanied by domain closure and substrate burial, as is the hallmark of ligand binding in periplasmic SBPs. The binding to the two carboxylates effectively forms a clamp around the ligand, projecting a substituent on the C2 carbon down towards the long inter-lobal β -strands (Figure 4A). We further identified a closely similar solved structure of PA0884 in complex with succinate (PDB: 9DTL) and aligned it with our structure of PA0884 bound to succinate, which has an RMSD of 0.325 Å (Supplementary Figure S3A,B). Unsurprisingly, these two ligands bind in a highly similar manner with V234, Q171, S91, K41, R169, K94, N209 and V34 contacts shared between them.

We then compared the structure of IctP with that of *P. aeruginosa* DctP (PA5167) bound to succinate (PDB: 9DSY) (Figure 6), a protein with a known function in succinate uptake in *P. aeruginosa* [20]. Secondary structure alignment of these three proteins shows absolute conservation of key binding site residues with the exception of V234 [34], reflecting the recent evolutionary relationship of these orthologous proteins (Figure 7). The alteration from the larger leucine residue in DctP to the smaller valine in IctP (Figure 6C) suggests that V234 could be the primary adaptation in IctP that enables it to recognise itaconate with µM affinity. In an identical binding site, the larger L234 residue found in DctP would likely interfere with the accommodation of itaconate in the binding.

Discussion

The role of short-chain dicarboxylates in the establishment of chronic *P. aeruginosa* infection in the lungs of individuals with pathologies like CF and COPD has long been known. While initially being recognised as part of the immune response to infections, short-chain dicarboxylates like succinate and itaconate are

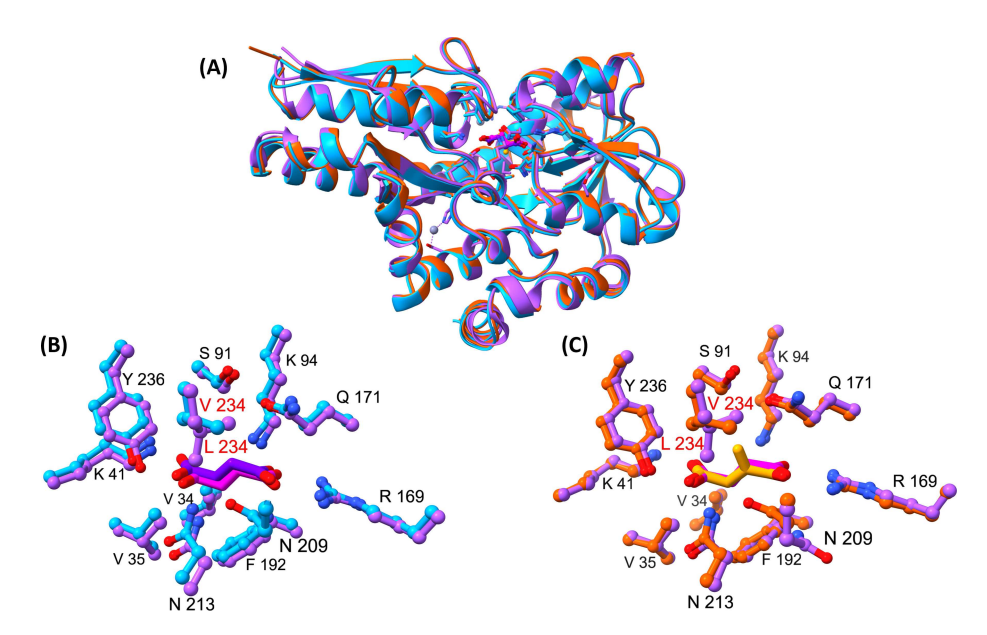


Figure 6: Structural comparison of IctP (PA0884) and DctP (PA5167) binding to itaconate and succinate.

(A) Overlay of PA0884 bound to succinate [9HT4] (cyan), PA0884 bound to itaconate (orange) [9HT3] and DctP (purple) bound to succinate (pink) [9DSY]. (B) A close-up view of the ligand-binding site of PA0884 (cyan) bound to succinate (purple) overlaid onto PA5167 (PDB ID: 9DSY) (purple) bound to succinate (pink). (C) A close-up view of the ligand-binding site of PA0884 (orange) bound to itaconate (yellow) overlaid onto DctP (purple) [9DSY] bound to succinate (pink).



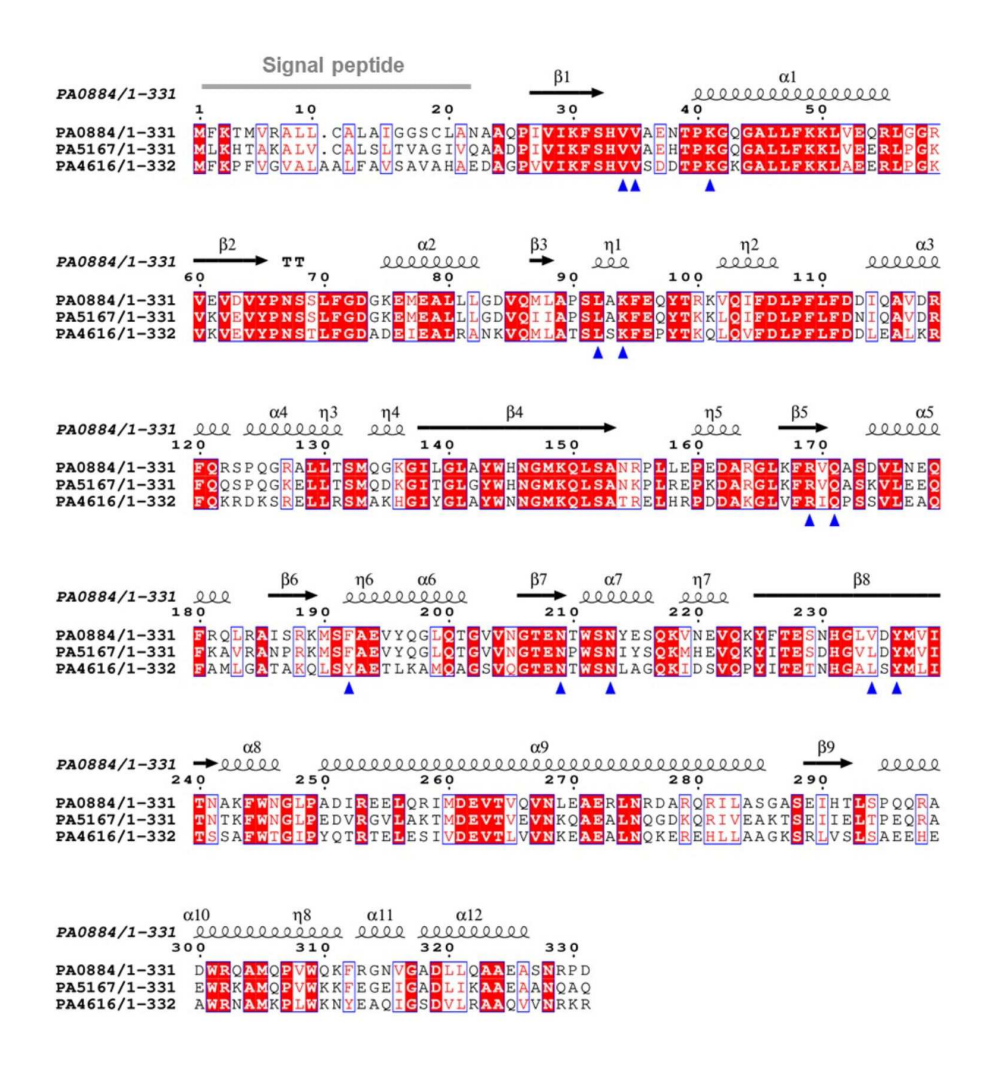


Figure 7: Sequence alignment of three PA01 TRAP SBPs with secondary structure template of PA0884 bound to succinate (9HT4).

ESPript alignment of PA0884, PA5167 and PA4616 highlighting secondary structures across the sequence (created using pdb 9HT4) and key binding site residues (blue triangles). V234 is the key binding site residue in PA0884, whereas L234 is well conserved in both PA5167 and PA4616. All the other key binding site residues are well conserved except F192. Created with ESPript.

now known to be used by the pathogen to reprogramme itself to allow persistence in the airway [17,18,35]. While there is some evidence for the function of DctA and DctPQM in succinate uptake [20], how itaconate was acquired was not known. The *pa0884–pa0886* genes were suggested to encode the transporter for itaconate due to their proximity to the itaconate catabolic genes [36], and there is evidence in the form of growth assays using heterologous expression of the entire *pa0878–pa0886* cluster to support this hypothesis [23]. In this study, we provide the first genetic evidence that these transporter genes, which we name *ictPQM*, are essential for itaconate uptake, and biochemical and structural data to suggest that IctP binds itaconate and also succinate and other dicarboxylates.

As *P. aeruginosa* PAO1 has a preference for succinate as a carbon source [37–39], it is perhaps not surprising that it can also utilise other dicarboxylates like itaconate as a sole carbon source, supporting comparable growth rates to succinate [20]. While for succinate there are multiple transporters of varying affinity that can take up succinate [20], our data suggest that the TRAP transporter is the sole route of uptake in *P. aeruginosa* PAO1 (Figure 1D). However, this genetic analysis revealed that while the small membrane component was essential for growth with itaconate, the disruption of the SBP did not completely abolish growth. This result is, on the one hand, a surprise, as the interactions between 'cognate' SBPs and their membrane components are usually unique, although in SBP-dependent ATP-binding cassette (ABC) transporters, there are examples of multiple SBPs interacting with the same membrane



domains [40]. On the other hand, given the high sequence similarity (73.6%) of the IctPQM system to the canonical DctPQM system, it is likely that the proteins are still similar enough for a 'non-cognate' interaction of a highly similar SBP, namely DctP (PA5167), with IctQM could occur, which is what we suggest is happening here. This is consistent also with our biochemical and structural data, which show the highly similar binding site between DctP and IctP and that C_4 -dicarboxylate binding is still retained in IctP. Examining the distribution of the IctPQM system, its presence in only a small number of related species of *Pseudomonas* clearly suggests that it has evolved via a duplication of the *dctPQM* genes in this lineage of bacteria and then subsequent specialisation towards itaconate as a substrate, although it clearly retains many of its 'ancestral' binding features.

TRAP transporters are interesting hybrid transporters that combine high ligand-binding affinity and specificity to concentrate substrates using the membrane potential, as opposed to via direct ATP hydrolysis as used by SBP-dependent ABC transporters [41,42]. It is interesting that while other 'scaffolds', such as the DctA C_4 -dicarboxylate transporter, are present in *Pseudomonas* sp., it has been the duplicated and adaptation of a TRAP system that has been selected during evolution, perhaps suggesting that the concentrations of itaconate in the environment where these more ancestral Pseudomonads evolved were in the low μ M range. The duplication of the SBP to confer additional binding range to a transporter has been seen multiple times in ABC transporters [43], but here, the duplication of the whole transporter and its integration into an itaconate-regulated operon [19] suggests that the bacteria have selected to genetically separate out the ancestral C_4 -dicarboxylate transport function to that of the new itaconate-specific IctPQM.

It is interesting to link this observation back to the role of itaconate transport and catabolism in infection biology. As *P. aeruginosa* likely had this functioning itaconate utilisation system before its specialisation as a human pathogen, it is possible that it helped enable successful host colonisation through the removal of this potentially toxic molecule. Thinking more broadly, considering that both in skin-wound settings and in the CF lung, the presence of *P. aeruginosa* is often found in polymicrobial CF infections [44,45], it is possible that the removal of itaconate by *P. aeruginosa* is a feature of these ecosystems. For example, *S. aureus* lung infections induce itaconate release in the airway through the activation of host *IrG1*[46], which is known to be bactericidal to *S. aureus* [47]. However, unlike *P. aeruginosa*, *S. aureus* is thought to be unable to degrade itaconate [48], so in a polymicrobial infection, it is possible that *P. aeruginosa* could alleviate the stress induced by itaconate for both itself and *S. aureus* by removing and degrading this molecule to allow persistence of both species in the airway.

While itaconate utilisation suggests a direct route to increased colonisation, there are also data suggesting a more indirect impact of external succinate and itaconate on the state of *P. aeruginosa* growth with studies suggesting that succinate inhibits biofilm formation, while another study suggestingthat itaconate promotes it [16,18]. To see if the lack of uptake due to loss of IctPQM function altered biofilm formation, an initial experiment suggested that itaconate, but not succinate, promoted biofilm formation in the absence of the transporter (Supplementary Figure S4). While it remains unclear what mechanisms are occurring here, it raises the possibility that itaconate is doing more than just being consumed by *P. aeruginosa* as a carbon and energy source, perhaps as a result of itaconate remaining outside the cell for a longer period of time prolonging outer membrane stress, which leads to increased biofilm formation.

In conclusion, our definition and analysis of the IctPQM TRAP transport system in this work reveal a lineage-specific duplication and specialisation of an ancestral C_4 -dicarboxylate transporter, DctPQM, for a function in itaconate uptake and the description of the first dedicated itaconate uptake system in bacteria.

Methods

Cloning and protein production

The SBP domain of the transporter operon pa0884 was cloned into pETYSBLIC3C [49] and expressed in $\it E.~coli~BL21(DE3)$. Cultivations were performed in baffled 2-l flasks on an orbital shaker at 120 rpm at 37°C. The 1-l expression cultures were set up in Lennox broth (LB) media with a starting optical density (OD) (600 nm) of 0.1 from overnight cultures. The expression cultures were induced with 0.5 mM isopropyl- β -D-thiogalactopyranoside (IPTG) at an OD 0.6 (at 600 nm). Overnight cultures were spun down, and cell pellets were resuspended in a 30-ml 20 mM KPi + 200 mM NaCl wash, 5 mM imidazole buffer and 10% glycerol. Resuspended cells were lysed with sonication, and clarified supernatant was collected by spinning down at 27000×g for 40 min at 4°C. Supernatant was loaded onto a 5-ml HisTrap Fast



Flow (FF) column (Cytiva) with an isocratic elution method with 20 mM KPi pH 8, 200 mM NaCl, 500 mM imidazole and 10% glycerol elution buffer using ÄKTA pure (Cytiva). Ni-affinity purification elution fractions were pooled together and loaded onto Supradex S-200 column (GE Healthcare Life Sciences, Buckinghamshire, U.K) for buffer exchange into size-exclusion chromatrography (SEC) buffer (20 mM Tris-HCl pH 8, 50 mM NaCl).

Protein melting temperature determination

NanoDSF was performed using Prometheus NanoTemper Technologies equipped with a back reflection mode (NanoTemper Technologies, München, Germany). The 10- μ l samples were loaded into the nanoDSF capillaries (NanoTemper Technologies, München, Germany) and placed in the sample holder. A final concentration of 5 μ M protein in 50 mM KPi, 200 mM NaCl and each ligand at final concentrations of 5 mM was analysed in triplicates. Ligands itaconic acid (CAS no. 97-65-4), succinic acid (CAS no. 110-15-6) and D-mannose (CAS no. 3458-28-4) were all sourced from Sigma Aldrich. The solutions for both itaconic acid and succinic acid were adjusted to pH 7 with NaOH making them into sodium salts. Samples were heated up at a thermal ramping rate of 1°C/min from 25 to 95°C, and intrinsic protein fluorescence was measured from 330 and 350 nm with a dual detector. The excitation power for the different samples varied, but was sufficient for A330 and A350 fluorescent signals to exceed 2000 relative fluorescence units. Protein melting temperature ($T_{\rm m}$) and aggregation (T_{agg}) were also calculated from the data and plotted in GraphPad (Prism 10).

Fluorimetry

Intrinsic tryptophan fluorescence was measured with the FluoroMax 4 fluorescence spectrometer (Horiba Jobin-Yvon) at room temperature. PA0884 was prepared in 50 mM KPi pH 7.8 with 200 mM NaCl buffer. The protein was used at a concentration of 0.5 μ M and excited at 295 nm with various ligands added at 100 μ M. The slit width was 3.5 nm, and the emission spectra were collected at 330 nm. Protein samples were titrated with increasing concentrations of ligands fumarate, malate, succinate and itaconate. K_D was calculated from the hyperbolic fit of the binding curve and plotted using GraphPad (Prism 10).

Crystallisation of PA0884-succinate and PA0884-itaconate

For crystallisation, recombinantly expressed PA0884 was concentrated to 15 mg/ml in 20 mM Tris-HCl pH 8, 50 mM NaCl and mixed with either 50 mM itaconate, pH 7 or 50 mM succinate and pH 7. The mixture was incubated in solution at room temperature for 15 min. Protein crystals were grown in sitting drops (1:1 ratio) over the crystallisation solution (JCSG-plus HT-96 D12: 0.04 M potassium phosphate monobasic, 16% w/v PEG 8000) at room temperature in MRC 96-well 2-drop crystallisation plates. Crystals of both protein–ligand complexes were cryo-protected using 20% glycerol.

Data collection and structure determination

X-ray diffraction data were collected at the Diamond Light Source, U.K on Beamline i03 for crystals of both PA0884-succinate and PA0884-itaconate. The data collected for both protein crystals were indexed and scaled using the DIALS pipeline [50]. Data reduction was performed using AIMLESS 0.7.13 [51]. The molecular replacement programme MOLREP [52] was used to obtain initial phase information for both protein crystals using the predicted structure of PA0884 generated using AlphaFold (AF-Q9I561-F1). The respective structures were refined using REFMAC5 [53]. Refined co-ordinate sets and structure factors were deposited into the PDB with the entry codes 9HT3 for PA0884-itaconate and 9HT4 for PA0884-succinate. Data collection statistics are provided in Supplementary Table S1.

Structural analysis

The buried surface area between the protein and ligand was calculated using the 'measure buried area' command in ChimeraX 1.8 [54]. The binding site was defined as atoms within 5 Å from the ligand. Solvent accessible surfaces were determined using a probe radius of 1.4 Å, which is used to approximate a water molecule. As a result, the buried surface area between the surface of the ligand and the surface of the surrounding protein residues could be determined.



Growth data

Strains used in the growth assays have the following genotypes: WT strain PAO1, enzymatic pathway mutant pa0878-E03::ISlacZ/hah, SBP domain pa0884-F06::ISlacZ/hah, small subunit of the membrane domain pa0885-C09::ISlacZ/hah and a gene of unrelated function as a negative control pa3728-C01::ISlacZ/hah. WT and mutant strains were grown overnight in LB media. Overnight cells were pelleted and washed with MilliQ water at 1000×g at 4°C. Cells were resuspended in Neidhart MOPS M9 minimal media with carbon sources itaconate, succinate, fumarate and D-glucose. Inoculation culture was added to Nunc™ MicroWell™ 96-well microplate wells to M9 minimal media and carbon sources.

Data Availability

Refined co-ordinate sets and structure factors were deposited into the PDB with the entry codes 9HT3 for PA0884-itaconate and 9HT4 for PA0884-succinate (54).

Competing Interests

All other authors declare that they have no conflicts of interest with the contents of this article.

Funding

This work was supported by the Biotechnology and Biological Sciences Research Council grant BB/W510373/1 supporting J.M., BB/W510531/1 supporting R. H, BB/T017805/1 for use of the X-ray facility and BB/X003035/1 for general support of the GHT lab.

CRediT Author Contribution

R. H., and G. H. T. conceptualization; J. M., R. H., R. C. E., and G. H. T. validation; J. M., R. H., B. K. W., R. C. E., A. J. W., and G. H. T. formal analysis; J. M., R. H., R. C. E., and G. H. T. investigation; J. M., R. H., B. K. W., R. C. E., H. A., A. J. W., and G. H. T. data curation; G. H. T. resources; J. M., R. H. writing—original draft; J. M., R. H., B. K. W., R. C. E., A. J. W., and G. H. T. writing—review & editing; J. M., R. H., B. K. W., and A. J. W. visualisation; A. J. W., M. W. vd W, and G. H. T. supervision; R. H., J. M., R. C. E., and G. H. T. project administration; A. J. W., and G. H. T. funding acquisition.

Acknowledgments

We thank Johan Turkenburg and Sam Hart for help with data collection and staff at the DIAMOND Light Source at Harwell for excellent X-ray facilities. We would also like to thank Dr Andrew Leech in the Technology Facility, Department of Biology, University of York for help with interpretation of data from nanoDSF and fluorimetry.

Abbreviations

CF, cystic fibrosis; COPD, chronic obstructive pulmonary disease; IPF, idiopathic pulmonary fibrosis; SBP, substrate-binding protein; TRAP, tripartite ATP-independent periplasmic; WT, wildtype; nanoDSF, nano differential scanning fluorimetry.

References

- Diggle, S.P. and Whiteley, M. (2020) Microbe profile: pseudomonas aeruginosa: opportunistic pathogen and lab rat. *Microbiology* (*Reading, Engl.*) **166**, 30–33 https://doi.org/10.1099/mic.0.000860
- 2 Lieberman, D. and Lieberman, D. (2003) Pseudomonal infections in patients with COPD: epidemiology and management. Am. J. Respir. Med. 2, 459–468 https://doi.org/10.1007/BF03256673 PMID: 14719985
- Magill, S.S., Edwards, J.R., Bamberg, W., Beldavs, Z.G., Dumyati, G., Kainer, M.A. et al. (2014) Multistate Point-Prevalence Survey of Health Care–Associated Infections. N. Engl. J. Med. 370, 1198–1208 https://doi.org/10.1056/NEJMoa1306801
- 4 Jesudason, T. (2024) WHO publishes updated list of bacterial priority pathogens. The Lancet Microbe 5, 100940 https://doi.org/10.1016/j.lanmic.2024.07.003
- 5 Yamazaki, R., Nishiyama, O., Sano, H., Iwanaga, T., Higashimoto, Y., Kume, H. et al. (2016) Clinical features and outcomes of ipf patients hospitalized for pulmonary infection: a japanese cohort study. *PLoS ONE* 11, e0168164 https://doi.org/10.1371/journal.pone.0168164
- 6 Burns, J.L., Gibson, R.L., McNamara, S., Yim, D., Emerson, J., Rosenfeld, M. et al. (2001) Longitudinal assessment of Pseudomonas aeruginosa in young children with cystic fibrosis. J. Infect. Dis. 183, 444–452 https://doi.org/10.1086/318075 PMID: 11133376



- 7 Tuli, J.F., Ramezanpour, M., Cooksley, C., Psaltis, A.J., Wormald, P.-J. and Vreugde, S. (2021) Association between mucosal barrier disruption by *Pseudomonas aeruginosa* exoproteins and asthma in patients with chronic rhinosinusitis. *Allergy* 76, 3459–3469 https://doi.org/10.1111/all.14959
- 8 Gallego, M., Pomares, X., Espasa, M., Castañer, E., Solé, M., Suárez, D. et al. (2014) Pseudomonas aeruginosaisolates in severe chronic obstructive pulmonary disease: characterization and risk factors. BMC Pulm. Med. 14, 103 https://doi.org/10.1186/1471-2466-14-103
- 9 Colvin, K.M., Irie, Y., Tart, C.S., Urbano, R., Whitney, J.C., Ryder, C, et al. (2012) The Pel and Psl polysaccharides provide Pseudomonas aeruginosa structural redundancy within the biofilm matrix: Polysaccharides of the P. aeruginosa biofilm matrix. Environ. Microbiol., Wiley 14, 1913–1928 https://doi.org/10.1111/j.1462-2920.2011.02657.x
- Malhotra, S., Hayes, D., Jr and Wozniak, D.J. (2019) Cystic fibrosis and pseudomonas aeruginosa: the host-microbe interface. Clin. Microbiol. Rev. 32 https://doi.org/10.1128/CMR.00138-18
- Siegel, L.S., Hylemon, P.B. and Phibbs, P.V., Jr. (1977) Cyclic adenosine 3',5'-monophosphate levels and activities of adenylate cyclase and cyclic adenosine 3',5'-monophosphate phosphodiesterase in Pseudomonas and Bacteroides. J. Bacteriol. 129, 87–96 https://doi.org/10.1128/jb.129.1.87-96.1977
- 12 Zhou, Y., Vazquez, A., Wise, A., Warita, T., Warita, K., Bar-Joseph, Z. et al. (2013) Carbon catabolite repression correlates with the maintenance of near invariant molecular crowding in proliferating E. coli cells. *BMC Syst. Biol.* **7**, 138 https://doi.org/10.1186/1752-0509-7-138
- 13 Pacheco, A.R., Curtis, M.M., Ritchie, J.M., Munera, D., Waldor, M.K., Moreira, C.G. et al. (2012) Fucose sensing regulates bacterial intestinal colonization. *Nature* 492, 113–117 https://doi.org/10.1038/nature11623
- 14 Guo, X.K., Wang, J., Van Hensbergen, V.P., Liu, J., Xu, H. and Hu, X. (2023) Interactions between host and intestinal crypt-resided biofilms are controlled by epithelial fucosylation. *Cell Rep.* **42**, 112754 https://doi.org/10.1016/j.celrep.2023.112754 PMID: 37405914
- 15 Bell, A., Brunt, J., Crost, E., Vaux, L., Nepravishta, R., Owen, C.D. et al. (2019) Elucidation of a sialic acid metabolism pathway in mucus-foraging Ruminococcus gnavus unravels mechanisms of bacterial adaptation to the gut. Nat. Microbiol. 4, 2393–2404 https://doi.org/10.1038/s41564-019-0590-7
- 16 Riquelme, S.A., Lozano, C., Moustafa, A.M., Liimatta, K., Tomlinson, K.L., Britto, C, et al. (2019) CFTR-PTEN-dependent mitochondrial metabolic dysfunction promotes airway infection. Sci. Transl. Med. 11 https://doi.org/10.1126/scitranslmed.aav4634
- 17 Riquelme, S.A. and Prince, A. (2020) Airway immunometabolites fuel Pseudomonas aeruginosa infection. *Respir. Res.* 21, 326 https://doi.org/10.1186/s12931-020-01591-x PMID: 33302964
- 18 Riquelme, S.A., Liimatta, K., Wong Fok Lung, T., Fields, B., Ahn, D., Chen, D, et al. (2020) Pseudomonas aeruginosa utilizes host-derived itaconate to redirect its metabolism to promote biofilm formation. *Cell Metab.* 31, 1091–1106 https://doi.org/10.1016/j.cmet.2020.04.017 PMID: 32428444
- Huang, Q., Duan, C., Ma, H., Nong, C., Zheng, Q., Zhou, J. et al. (2024) Structural and functional characterization of itaconyl-CoA hydratase and citramalyl-CoA lyase involved in itaconate metabolism of Pseudomonas aeruginosa. Structure 32, 941–952 https://doi.org/10.1016/j.str.2024.04.004 PMID: 38677288
- 20 Valentini, M., Storelli, N. and Lapouge, K. (2011) American Society for Microbiology1752 N St., N.W., Washington, DC 193. J. Bacteriol. 4307–4316 https://doi.org/10.1128/JB.05074-11/SUPPL_FILE/TABLES1.DOC
- 21 Thomas, G.H., Southworth, T., León-Kempis, M.R., Leech, A. and Kelly, D.J. (2006) Novel ligands for the extracellular solute receptors of two bacterial TRAP transporters. *Microbiology (Reading, Engl.)* 152, 187–198 https://doi.org/10.1099/mic.0.28334-0
- 22 Sasikaran, J., Ziemski, M., Zadora, P.K., Fleig, A. and Berg, I.A. (2014) Bacterial itaconate degradation promotes pathogenicity. *Nat. Chem. Biol.* **10**, 371–377 https://doi.org/10.1038/nchembio.1482
- 23 De Witt, J., Ernst, P., G\u00e4tgens, J., Noack, S., Hiller, D., Wynands, B, et al. (2023) Characterization and engineering of branched short-chain dicarboxylate metabolism in Pseudomonas reveals resistance to fungal 2-hydroxyparaconate. Metab. Eng. 75, 205–216 https://doi.org/10.1016/j.ymben.2022.12.008
- Wolff, J.A., MacGregor, C.H., Eisenberg, R.C. and Phibbs, P.V., Jr. (1991) Isolation and characterization of catabolite repression control mutants of Pseudomonas aeruginosa PAO. *J. Bacteriol.* **173**, 4700–4706 https://doi.org/10.1128/jb.173.15.4700-4706.1991
- Valentini, M. and Lapouge, K. (2013) Catabolite repression in Pseudomonas aeruginosa PAO1 regulates the uptake of C4 -dicarboxylates depending on succinate concentration: Succinate concentrations tune Crc regulation of
- Herman, R., Mehboob, J., Elsto, R. and Afolabi, H. (2025) Crystal structure of PA0884, the SBP component of a Pseudomonas aeruginosa PAO1 Tripartite ATP-independent Periplasmic (TRAP) transporter, complexed with succinate.https://www.wwpdb.org/pdb?id=odb_00009ht4
- 27 Peter, M.F., Ruland, J.A., Kim, Y., Hendricks, P., Schneberger, N., Siebrasse, J.P. et al. (2024) Conformational coupling of the sialic acid TRAP transporter HiSiaQM with its substrate binding protein HiSiaP. *Nat. Commun.* 15, 217 https://doi.org/10.1038/ s41467-023-44327-3 PMID: 38191530
- King-Hudson, T.-R.J., Davies, J.S., Quan, S., Currie, M.J., Tillett, Z.D., Copping, J. et al. (2024) On the function of TRAP substrate-binding proteins: conformational variation of the sialic acid binding protein SiaP. *Journal of Biological Chemistry* 300, 107851 https://doi.org/10.1016/j.jbc.2024.107851
- 29 Chandravanshi, M., Tripathi, S.K. and Kanaujia, S.P. (2021) An updated classification and mechanistic insights into ligand binding of the substrate-binding proteins. FEBS Lett. 595, 2395–2409 https://doi.org/10.1002/1873-3468.14174
- 30 Bisson, C., Salmon, R.C., West, L., Rafferty, J.B., Hitchcock, A., Thomas, G.H. et al. (2022) The structural basis for high-affinity uptake of lignin-derived aromatic compounds by proteobacterial TRAP transporters. FEBS J. 289, 436–456 https://doi.org/10.1111/febs.16156 PMID: 34375507
- 31 Schneberger, N., Hendricks, P., Peter, M.F., Gehrke, E., Binder, S.C., Koenig, P.-A. et al. (2024) Allosteric substrate release by a sialic acid TRAP transporter substrate binding protein. *Commun. Biol.* 7, 1559 https://doi.org/10.1038/s42003-024-07263-6
- Fischer, M., Zhang, Q.Y., Hubbard, R.E. and Thomas, G.H. (2010) Caught in a TRAP: substrate-binding proteins in secondary transport. Trends Microbiol. 18, 471–478 https://doi.org/10.1016/j.tim.2010.06.009 PMID: 20656493



- Fischer, M., Hopkins, A.P., Severi, E., Hawkhead, J., Bawdon, D., Watts, A.G. et al. (2015) Tripartite ATP-independent Periplasmic (TRAP) Transporters Use an Arginine-mediated Selectivity Filter for High Affinity Substrate Binding. *Journal of Biological Chemistry* **290**, 27113–27123 https://doi.org/10.1074/jbc.M115.656603
- Gouet, P., Robert, X. and Courcelle, E. (2003) ESPript/ENDscript: Extracting and rendering sequence and 3D information from atomic structures of proteins. *Nucleic Acids Res.* 31, 3320–3323 https://doi.org/10.1093/nar/gkq556 PMID: 12824317
- Tramper-Stranders, G.A., Molin, S., Yang, L., Hansen, S.K., Rau, M.H, et al. (2012) Initial Pseudomonas aeruginosa infection in patients with cystic fibrosis: characteristics of eradicated and persistent isolates. *Clin. Microbiol. Infect.* **18**, 567–574 https://doi.org/10.1111/i.1469-0691.2011.03627.x
- D'Arpa, P., Karna, S.L.R., Chen, T. and Leung, K.P. (2021) Pseudomonas aeruginosa transcriptome adaptations from colonization to biofilm infection of skin wounds. *Sci. Rep.* **11**, 20632 https://doi.org/10.1038/s41598-021-00073-4 PMID: 34667187
- 37 Collier, D.N., Hager, P.W. and Phibbs, P.V., Jr. (1996) Catabolite repression control in the Pseudomonads. *Res. Microbiol.* **147**, 551–561 https://doi.org/10.1016/0923-2508(96)84011-3 PMID: 9084769
- 38 Görke, B. and Stülke, J. (2008) Carbon catabolite repression in bacteria: many ways to make the most out of nutrients. *Nat. Rev. Microbiol.* **6**, 613–624 https://doi.org/10.1038/nrmicro1932 PMID: 18628769
- Rojo, F. (2010) Carbon catabolite repression in Pseudomonas: optimizing metabolic versatility and interactions with the environment. FEMS Microbiol. Rev. 34, 658–684 https://doi.org/10.1111/j.1574-6976.2010.00218.x PMID: 20412307
- Thomas, G.H. (2010) Homes for the orphans: utilization of multiple substrate-binding proteins by ABC transporters. *Mol. Microbiol.* **75**, 6–9 https://doi.org/10.1111/j.1365-2958.2009.06961.x
- 41 Mulligan, C., Fischer, M., Thomas, G.H., and Oxford University Press (OUP) 35. (2011) Tripartite ATP-independent periplasmic (TRAP) transporters in bacteria and archaea. FEMS Microbiol. Rev. 35, 68–86 https://doi.org/10.1111/j.1574-6976.2010.00236.x PMID: 20584082
- 42 Rosa, L.T., Bianconi, M.E., Thomas, G.H. and Kelly, D.J. (2018) Tripartite ATP-Independent Periplasmic (TRAP) Transporters and Tripartite Tricarboxylate Transporters (TTT): From Uptake to Pathogenicity. Front. Cell. Infect. Microbiol. 8, 33 https://doi.org/10.3389/fcimb.2018.00033
- 43 Maqbool, A., Levdikov, V.M., Blagova, E.V., Hervé, M., Horler, R.S.P., Wilkinson, A.J. et al. (2011) Compensating stereochemical changes allow murein tripeptide to be accommodated in a conventional peptide-binding protein. J. Biol. Chem. 286, 31512–31521 https:// doi.org/10.1074/jbc.M111.267179 PMID: 21705338
- 44 Sibley, C.D., Rabin, H. and Surette, M.G. (2006) Cystic fibrosis: a polymicrobial infectious disease. *Future Microbiol.* **1**, 53–61 https://doi.org/10.2217/17460913.1.1.53 PMID: 17661685
- 45 Bisht, K., Baishya, J. and Wakeman, C.A. (2020) Pseudomonas aeruginosa polymicrobial interactions during lung infection. *Curr. Opin. Microbiol.* **53**, 1–8 https://doi.org/10.1016/j.mib.2020.01.014 PMID: 32062024
- 46 Tomlinson, K.L., Lung, T.W.F., Dach, F., Annavajhala, M.K., Gabryszewski, S.J., Groves, R.A. et al. (2021) Staphylococcus aureus induces an itaconate-dominated immunometabolic response that drives biofilm formation. *Nat. Commun.* **12**, 1399 https://doi.org/10.1038/s41467-021-21718-y
- 47 Naujoks, J., Tabeling, C., Dill, B.D., Hoffmann, C., Brown, A.S., Kunze, M. et al. (2016) IFNs Modify the Proteome of Legionella-Containing Vacuoles and Restrict Infection Via IRG1-Derived Itaconic Acid. *PLoS Pathog.* 12, e1005408 https://doi.org/10.1371/journal.ppat.1005408 PMID: 26829557
- 48 Tomlinson, K.L. and Riquelme, S.A. (2021) Host-bacteria metabolic crosstalk drives S. aureus biofilm. *Microb. Cell* **8**, 106–107 https://doi.org/10.15698/mic2021.05.749
- 49 Fogg, M.J. and Wilkinson, A.J. (2008) Higher-throughput approaches to crystallization and crystal structure determination. *Biochem. Soc. Trans.* 36, 771–775 https://doi.org/10.1042/BST0360771 PMID: 18631156
- 50 Winter, G., Waterman, D.G., Parkhurst, J.M., Brewster, A.S., Gildea, R.J., Gerstel, M. et al. (2018) DIALS: implementation and evaluation of a new integration package. Acta Crystallogr. D. Struct. Biol. 74, 85–97 https://doi.org/10.1107/S2059798317017235
- 51 Evans, P.R. and Murshudov, G.N. (2013) How good are my data and what is the resolution? *Acta Crystallogr. D Biol. Crystallogr.* **69**, 1204–1214 https://doi.org/10.1107/S0907444913000061
- 52 Vagin, A. and Teplyakov, A. (1997) MOLREP: an automated program for molecular replacement. J. Appl. Crystallogr. 30, 1022–1025 https://doi.org/10.1107/S0021889897006766
- 53 Murshudov, G.N., Skubák, P., Lebedev, A.A., Pannu, N.S., Steiner, R.A., Nicholls, R.A. et al. (2011) REFMAC 5 for the refinement of macromolecular crystal structures. Acta Crystallogr. D Biol. Crystallogr. 67, 355–367 https://doi.org/10.1107/S0907444911001314
- 54 Pettersen, E.F., Goddard, T.D., Huang, C.C., Meng, E.C., Couch, G.S., Croll, T.I. et al. (2021) UCSF ChimeraX: Structure visualization for researchers, educators, and developers. *Protein Sci.* 30, 70–82 https://doi.org/10.1002/pro.3943 PMID: 32881101